

RESEARCH MEMORANDUM

FORCE MEASUREMENTS ON CONE-CYLINDER BODY OF REVOLUTION
WITH VARIOUS NOSE AND FIN CONFIGURATIONS
AT MACH NUMBER 4.0

By Leonard Rabb and Wesley E. Messing

Lewis Flight Propulsion Laboratory
Cleveland, Ohio

CLASSIFICATION CHANGED TO UNCLASSIFIED
AUTHORITY: NASA PUBLICATION ANNOUNCEMENT NO. 4
EFFECTIVE DATE: FEBRUARY 10, 1959

Restriction/Classification Cancelled

CLASSIFIED DOCUMENT

of the espionage laws, Title 18, U.S.C., Secs. 793 and 794, the transmission or revelation of which in any manner to an unauthorized person is prohibited by law.

NATIONAL ADVISORY COMMITTEE FOR AERONAUTICS

WASHINGTON

March 12, 1954

CONFIDENTIAL

Restriction/Classification
Cancelled

NATIONAL ADVISORY COMMITTEE FOR AERONAUTICS

RESEARCH MEMORANDUMFORCE MEASUREMENTS ON CONE-CYLINDER BODY OF REVOLUTION WITH
VARIOUS NOSE AND FIN CONFIGURATIONS AT MACH NUMBER 4.0

By Leonard Rabb and Wesley E. Messing

SUMMARY

An investigation was made to determine the effects of six stabilizing fin plan forms and three body-nose configurations on the static stability of a 20° cone-cylinder body of revolution that had a fineness ratio of 8.65. The fin plan forms tested were swept untapered fins with 45° and 60° sweep angles, trapezoidal fins, and delta fins. The nose configurations tested were conical, conical with a protruding antenna, and conical with a single-oblique-shock type supersonic inlet attached to the nose. The tests were conducted in the NACA Lewis 2- by 2-foot supersonic wind tunnel at a Mach number of 4.0 and a Reynolds number of 1.1×10^6 per foot.

Normal force coefficients, pitching moment coefficients, and center of pressure locations are presented at angles of attack up to 4° . Also presented are the center of pressure locations and the incremental normal force coefficients of the fins in the presence of the body. It was shown that the addition of either a single-cone supersonic inlet or a long antenna-type boom ahead of the body did not materially affect the center of pressure location of the complete fin-body configuration at angles of attack up to 4° .

The slope of the normal force coefficient curve at 0° angle of attack was 0.076 per degree for the cone-cylinder body without fins. For the same body in the presence of the antenna-type boom and the supersonic inlet, the slopes of the normal force coefficient curve were 0.072 and 0.035 per degree, respectively.

INTRODUCTION

It is generally recognized that the stability problem associated with fin-stabilized supersonic missiles and research test vehicles is intensified by an increase in flight Mach number. The unstable moment

contribution of the body remains nearly constant with increasing Mach number, but the decrease in fin effectiveness with increasing Mach number results in a decrease in the over-all stability. Consequently, a configuration which has stability at low supersonic velocities may become unstable at higher speeds. The design of a missile to be stable over a range of supersonic Mach numbers therefore necessitates providing an adequate distance between the center of pressure and the center of gravity at the peak velocities. This may be achieved aerodynamically by a proper choice of fin area and plan form.

The wind tunnel investigation described in this report was conducted with a 0.378 scale model of the research test vehicle described in reference 1. The purpose of the investigation was to establish the center of pressure locations for the various proposed configurations so that the stability of the full-scale test vehicle could be accurately predicted at high Mach numbers if the center of gravity were known. Figure 1 illustrates the cone cylinder body used in this investigation as well as the six proposed fin plan forms and three nose configurations.

Because the free-flight research vehicle could provide a technique for obtaining transient inlet data through a high Mach number and Reynolds number range, it was of interest to determine the effect of the addition of a single-cone supersonic inlet attached to the nose of the wind tunnel model on the static stability. In addition, the center of pressure was determined for the cone-cylinder configuration with a boom-type antenna affixed to the nose. Figure 2 illustrates the various nose configurations tested. The results of this investigation obtained at a Mach number of 4.0 through an angle of attack range of 0° to 4° are reported herein.

SYMBOLS

The following symbols are used in this report:

- C_M pitching moment coefficient about apex of cone, $M/q_0 S l$
- C_N normal force coefficient, $N/q_0 S$
- C_{N_α} slope of curve of normal force coefficient against angle of attack at 0°
- l body length, ft (2.52)
- M moment about apex of cone, ft-lb
- M_0 free-stream Mach number

N normal force, lb

p_0 free-stream static pressure, lb/sq ft

q_0 free-stream dynamic pressure, $0.7 p_0 M_0^2$, lb/sq ft

S maximum body cross-sectional area, sq ft (0.0668)

ΔC_N incremental normal force coefficient of fins, $C_{N_{FB}} - C_{N_B}$

α angle of attack, deg

Subscripts:

B body without fins

FB fin-body combination

APPARATUS AND PROCEDURE

The investigation was conducted in the NACA Lewis 2- by 2-foot supersonic wind tunnel, which is a nonreturn-type tunnel having a Reynolds number of 1.1×10^6 per foot and a test section Mach number of 4.00 ± 0.04 . The total temperature was maintained at approximately 200°F .

The model investigated consisted of a 20° cone-cylinder body of revolution having a fineness ratio of 8.65 and a body diameter of 3.50 inches. It was supported in the tunnel by a sting extending upstream from a vertical strut mounted on the top of the tunnel (fig. 3). The model was designed so that the various nose configurations and fins could be easily changed without removing the model from the tunnel. The dimensions of the model components are presented in figures 4 and 5. The different noses for the body are designated 1, 2, and 3, while the fins are noted by the letters A through F. In the discussion that follows, the configurations may be referred to by number and letter. For example, the basic cone-cylinder body in combination with nose number 1 and fin A may be called 1-A. In reference to the body configuration without fins, the letter X will be used and the configuration will be called 1-X.

The single-cone inlet used as one of the nose configurations was designed for the conical shock to intercept the cowl lip at a Mach number of 3.85. The frontal area of this inlet was 35 percent of the test body frontal area.

The lift, drag, and pitching moment were measured by means of a three component flexure-type strain-gage balance which was rigidly mounted

to the sting and to the inside of the model. The cruciform fin configuration was oriented so that two of the fins were in a plane perpendicular to the angle of attack plane. The tests were conducted at angles of attack of 4° or less because of the limitations of the pitching moment strain gage.

RESULTS AND DISCUSSION

Normal Force Coefficient

The normal force coefficient of the basic body (without fins) C_{NB} is presented in figure 6 for the three nose configurations tested as a function of the angle of attack. At a given angle of attack, the highest value of C_{NB} was obtained with configuration 1-X (20° cone), while a slightly lower value was obtained with 2-X (attached boom-antenna). Nose 3, which consisted of a single-cone supersonic inlet attached to the forebody, caused an appreciable loss in the body normal force coefficient. At 4° angle of attack, C_{NB} for configuration 3-X was approximately 65 percent of the value of the other two tips. Figure 6 also shows the normal force coefficient of the body without fins for configuration 1-X as computed from reference 2, which is a correlation of other experimental data, and from the semiempirical method given in reference 3. Both these references predict lower values of C_{NB} than the data obtained for 1-X. At 4° angle of attack, the experimental C_{NB} for configuration 1-X was 0.303 as compared with 0.250 from reference 2 and 0.170 from reference 3. The normal force curve slopes at zero angle of attack $C_{N\alpha}$ were 0.076 and 0.072 for configurations 1-X and 2-X, respectively, and the slope was only 0.035 for 3-X.

The normal force coefficients for all the fin-body combinations tested are shown in figure 7. The slopes of the normal force coefficient curves at zero angle of attack are also noted. In addition, the normal force coefficients of the complete fin-body combinations as predicted by the combined methods of references 2, 4, and 5 are given for fins in combination with nose 1 (fig. 7(a)). For a typical case, configuration 1-C, the theoretical value of the normal force coefficient is 86 percent of the experimentally measured value at an angle of attack of 4° .

The data of figure 7 are also presented in figure 8 in the form of $C_{N\alpha}$ against fin area. From figure 8, it can be seen that the loss of the body normal force due to the addition of the supersonic inlet (as shown in fig. 6) is reflected in the lower values of $C_{N\alpha}$ for the fin-body combination. The agreement between the data for nose configurations

1 and 2 is as expected since the values of the normal force coefficients for the body alone were similar. For fins of equal area but different plan forms, no significant change in $C_{N\alpha}$ could be noted, and it appears that for a given nose configuration $C_{N\alpha}$ was a linear function of fin area only.

The incremental normal force coefficient ΔC_N is the contribution to the over-all normal force coefficient provided by the fins in the presence of a body and is presented in figure 9. Each data point was obtained by subtracting the normal force coefficient of the body without fins from the normal force coefficient of the complete fin-body configuration at corresponding angles of attack and for identical nose configurations. Also shown are the theoretical normal force coefficients of the fins alone from reference 4. The interference effect of the body on the fins as given by Stewart and Meghreblian in reference 5 was applied to the fin normal force coefficients of the fins alone as obtained from reference 4 in order to predict ΔC_N . This interference factor is a function of fin plan form and of the ratio of body diameter to fin span (including the body). It is based on the theoretical work of Beskin (ref. 6). The theoretical values of ΔC_N as predicted in reference 4 and modified by the method of reference 5 are in good agreement with the data for each of the fins tested.

Pitching Moment Coefficient

The pitching moment coefficient C_M based on the body length and on the moment about the apex of the cone is presented in figure 10 as a function of C_N . The configurations are grouped according to the nose configuration so that the data for noses 1, 2, and 3 are given in figures 9(a), 9(b), and 9(c), respectively. The slope of the curve (dC_M/dC_N) is a measure of the stability, and the slope is greatest for fin E, which has the largest fin area and sweep angle and consequently would be expected to have the greatest stability.

Center of Pressure

Figure 11 presents the center of pressure (in body lengths from the cone apex) as a function of angle of attack for the bodies without fins as well as for the fin-body combinations. Included in figure 11(a) are the centers of pressure as predicted for the body without fins (refs. 2 and 3) and as calculated for the fin-body combinations based on references

2, 4, and 5. The calculated center of pressure locations for the fin-body combinations assumed the center of pressure of the fin force to be at the centroid of the fin area. The disagreement between the experimental center of pressure of the body without fins and as predicted by reference 2 amounted to approximately 7 percent of the body length at 3° angle of attack. Reference 3 showed an even larger difference.

Even though the data of reference 2 predicted the center of pressure of the body without fins to be further forward than it actually was, the center of pressure of the fin-body combination showed excellent agreement between the data and the location predicted by references 2, 4, and 5. This apparent discrepancy was resolved because the predicted normal force coefficient of the body without fins was less than the measured value (fig. 6). The combined effect of a smaller C_N and further forward center of pressure location for the body without fins was compensating. The predicted center of pressure for the fin-body combinations of nose 1 would therefore be expected to agree with the data, since the predicted fin forces have previously been shown to be in good agreement with the data (fig. 9).

Figure 11(b) presents the experimentally determined center of pressure for the nose 2 configurations. The calculation of the center of pressure of the body without fins was based on the experimental data of figures 6, 7(b), 9, and 11(b).

The centers of pressure for the nose 3 configurations are presented in figure 11(c). In contrast with the data for body noses 1 and 2, there was a decided forward shift in the center of pressure as the angle of attack increased. The shift was not observed for the body without fins (3-X), which remained constant at a center of pressure equal to 0.3127. Consequently, the movement of the center of pressure of the fin-body combination was attributed to the nonlinearity of the normal force coefficient curve for the body without fins, as shown in figure 6 for configuration 3-X.

In order to show the effects of the various nose configurations on the center of pressure of a typical fin-body configuration as well as the effect of the noses on the center of pressure of a body without fins, the data for the three body configurations without fins and with fin C are replotted in figure 12. The centers of pressure for configurations 1-X and 2-X are nearly identical and show a slight rearward movement (center of pressure = 0.4157 to 0.4607) as the angle of attack increases from 1° to 4° . The center of pressure location for configuration 3-X was considerably nearer the nose and remained constant with an increasing angle of attack at 0.3127. The center of pressure for the fin-stabilized configurations involving the three different nose configurations do not differ greatly at 4° angle of attack. The configuration which has the ram-jet inlet ahead of the body has the greatest stability followed

closely by the cone and the long antenna-nose configurations. This results from the fact that the normal force coefficient for configuration 3-X is much less than that for either 1-X or 2-X (fig. 6) and more than compensates for the difference in the center of pressure location of the body alone.

The location of the center of pressure of the fins is presented in figure 13 against the centroid of the fin plan forms. Each data point represents the average of all the test points for a given fin, and the solid line represents the line of perfect agreement between the center of pressure of the fins and the fin centroids. Although the fin center of pressure may be affected by the location of the fins on the body, the data show excellent agreement of fin center of pressure and fin centroid.

CONCLUDING REMARKS

It has been shown that for a cone-cylinder configuration with a fixed center of gravity the greatest margin of stability (distance between the center of gravity and center of pressure) would be encountered with fin E, which had the greatest sweep angle and fin area. However, the aerodynamic forces encountered by the fins during the wind tunnel investigation were sufficiently small as to preclude any aeroelastic effects despite the large sweep angle of fin E. In the selection of a fin plan form for a proposed cone-cylinder test vehicle which would operate under conditions of extremely high aerodynamic forces at a Mach number of 5.0, serious consideration must be given to the aeroelasticity of the fins. In order to provide adequate rigidity, fin E would necessarily be extremely thick and heavy, which for this particular test vehicle seriously reduced the margin of stability by moving the center of gravity rearward. This consideration led to the selection of the trapezoidal fin (fin C). The distance between the center of gravity of the flight vehicle and the center of pressure as determined from this wind tunnel investigation was 0.087 body length at a Mach number of 4.0. This margin proved adequate as the test vehicle was successfully rocket-boosted to a maximum Mach number of 5.18 (ref. 1).

CONCLUSIONS

The following conclusions were drawn from an investigation made to determine the effects of various fin plan forms and nose configurations on the center of pressure of a cone-cylinder body of revolution of fineness ratio 8.65 at a Mach number of 4.00:

1. The forces acting on the fins in the presence of the test body can be predicted by modifying the theoretical forces of the fins alone by the body interaction effects as suggested by Stewart and Meghreblian.

2. The center of pressure for the fins in the presence of the test body may be considered to act at the centroid of the fin area.

3. The slope of the normal force coefficient curve at zero angle of attack for a fin-stabilized body was not affected by the fin plan form but was a linear function of fin area.

4. The addition of a single-cone supersonic inlet to the basic cone-cylinder body produces a considerable loss of normal force on the body without fins. The slope of the normal force coefficient curve at zero angle of attack was reduced from 0.076 to 0.035, and the center of pressure was 0.312 of the body length at 3° angle of attack.

5. The addition of a long antenna-type boom ahead of the cone-cylinder configuration does not appreciably alter the aerodynamic characteristics of either the body without fins or the body in combination with the fins for the angles of attack tested. The slope of the normal force coefficient curve at zero angle of attack was 0.072 for the body without fins.

6. The center of pressure for the fin-stabilized configurations involving the three different nose configurations do not differ greatly at 4° angle of attack. The configuration which has the ram-jet inlet ahead of the body has the greatest stability followed closely by the cone and the long antenna-nose configurations.

Lewis Flight Propulsion Laboratory
National Advisory Committee for Aeronautics
Cleveland, Ohio, January 4, 1954

REFERENCES

1. Messing, Wesley E., Rabb, Leonard, and Disher, John H.: Preliminary Drag and Heat-Transfer Data Obtained from Air-Launched Cone-Cylinder Test Vehicle over Mach Number Range from 1.5 to 5.18. NACA RM E53IO4, 1953.
2. Grimminger, G., Williams, E. P., and Young, G. B. W.: Lift on Inclined Bodies of Revolution in Hypersonic Flow. Jour. Aero. Sci., vol. 17, no. 11, Nov. 1950, pp. 675-690.

3. Allen, H. Julian: Estimation of the Forces and Moments Acting on Inclined Bodies of Revolution of High Fineness Ratio. NACA RM A9I26, 1949.
4. Piland, Robert O.: Summary of the Theoretical Lift, Damping-in-Roll, and Center-of-Pressure Characteristics of Various Wing Plan Forms at Supersonic Speeds. NACA TN 1977, 1949.
5. Stewart, Homer J., and Meghreblan, Robert V.: Body-Wing Interference in Supersonic Flow. Prog. Rep. No. 4-99, Jet Prop. Lab., C.I.T., June 2, 1949.
6. Beskin, L.: Determination of Upwash Around a Body of Revolution at Supersonic Velocities. Rep. No. CM-251, Appl. Phys. Lab., Johns Hopkins Univ., May 27, 1946.

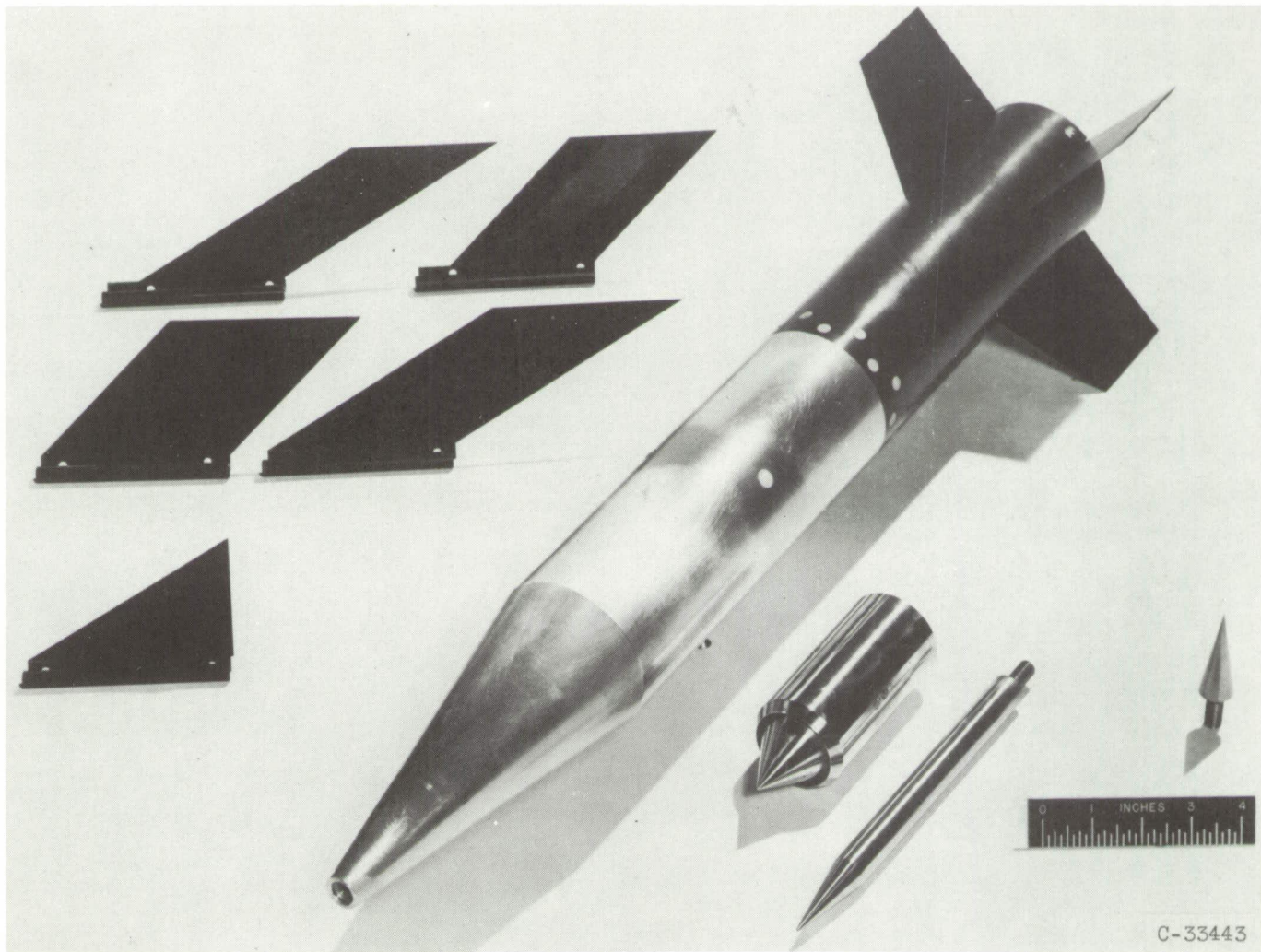
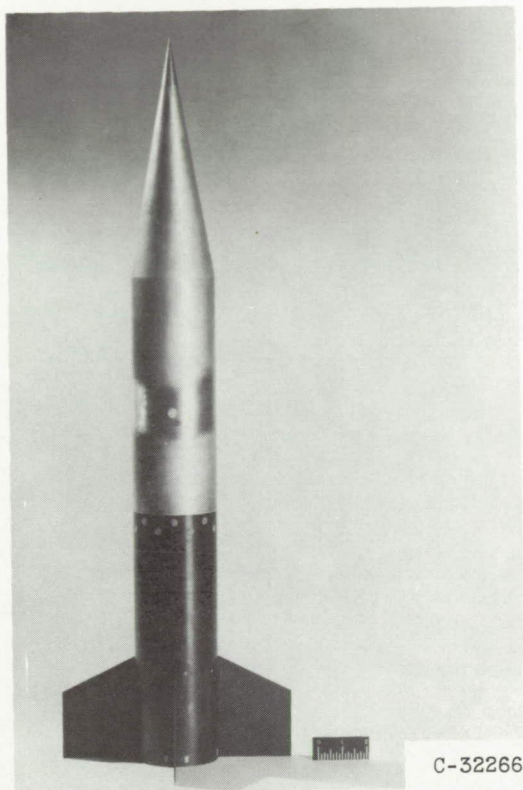
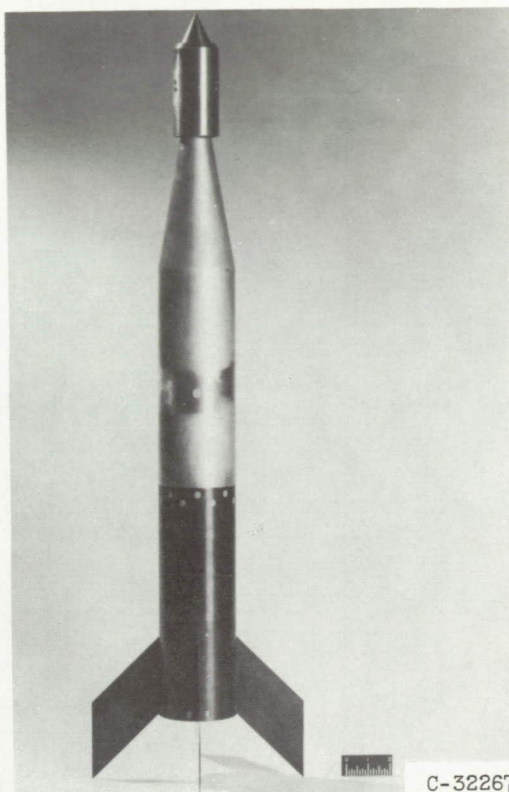


Figure 1. - Photograph of model including different fins and nose configurations tested.



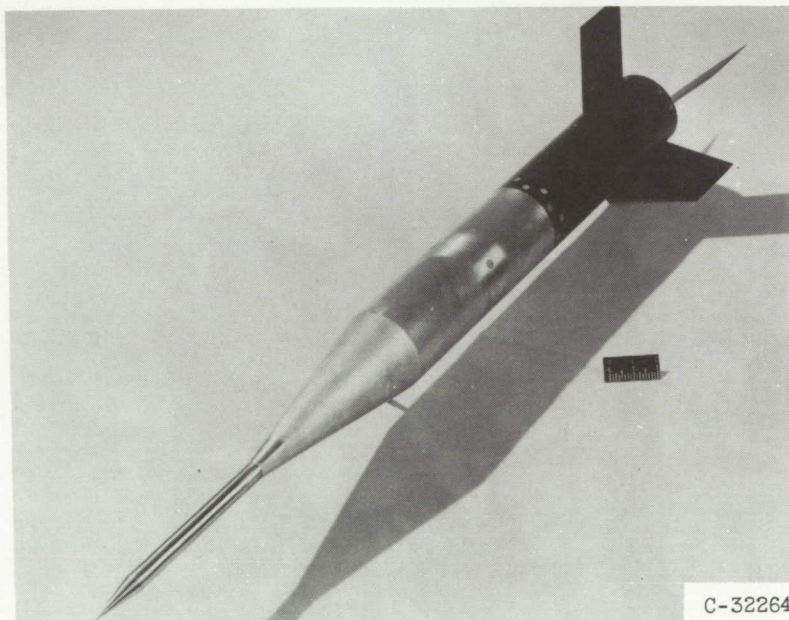
C-32266

(a) Conical tip.



C-32267

(b) Single-oblique-shock type inlet.



C-32264

(c) Conical tip with protruding antenna.

Figure 2. - Various nose configurations.

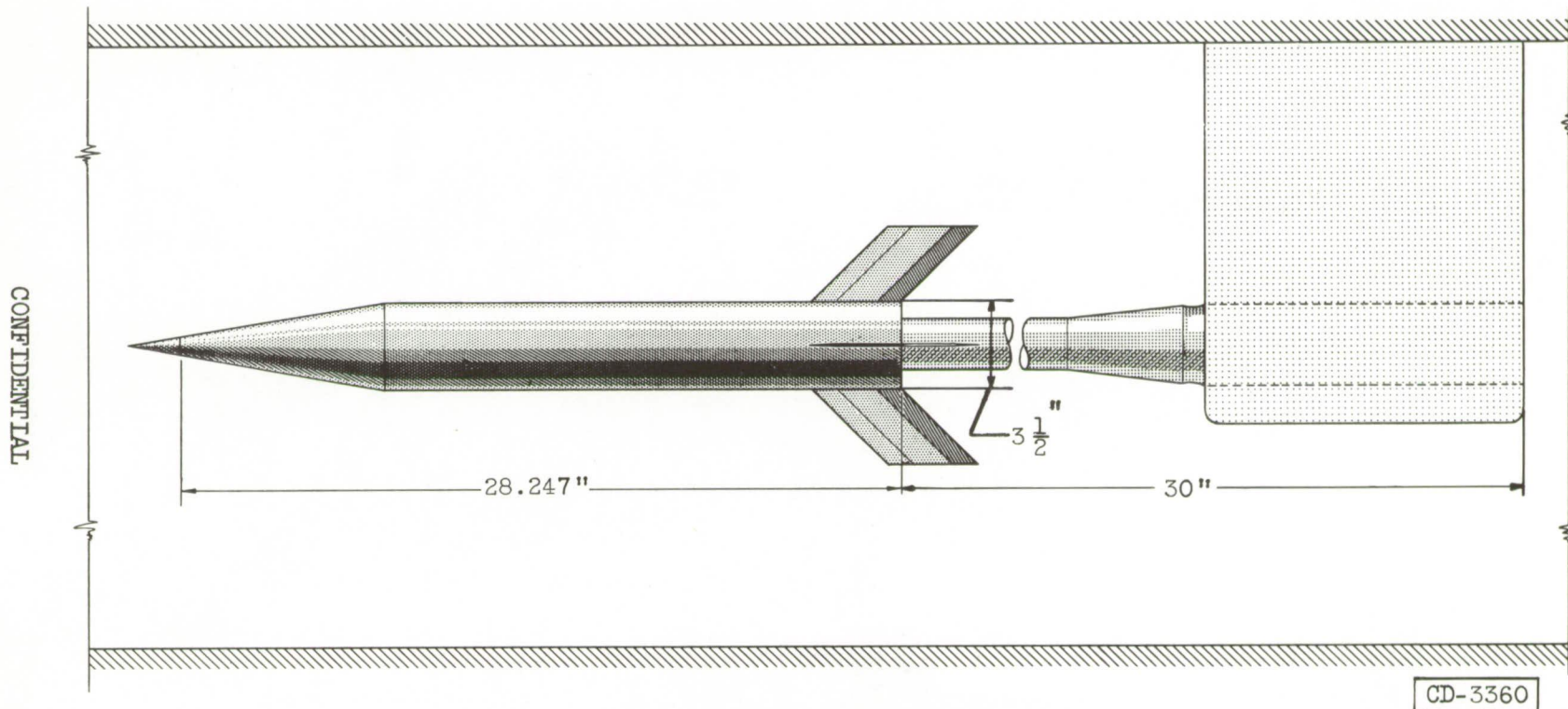
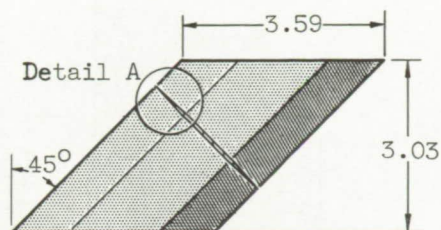
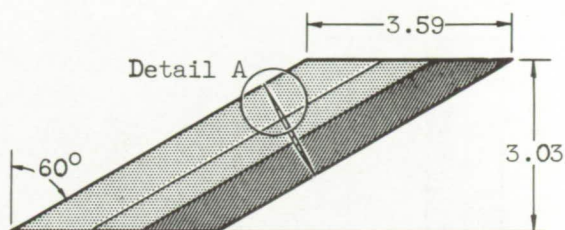


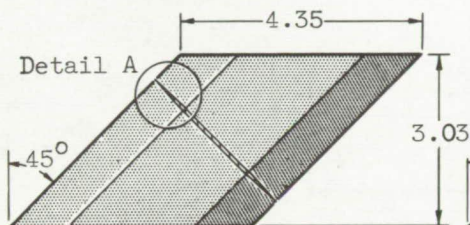
Figure 3. - Sketch of test model as mounted in 2- by 2-foot tunnel.



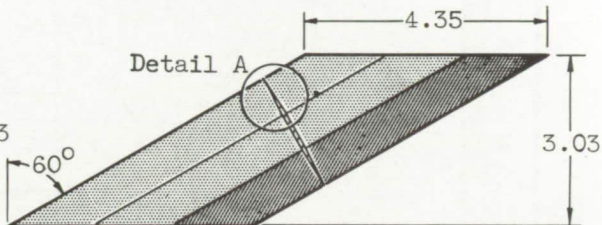
Fin A; fin area, 10.88;
aspect ratio, 1.69.



Fin B; fin area, 10.88;
aspect ratio, 1.69.

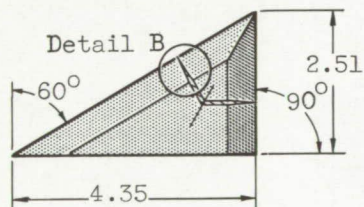


Fin D; fin area, 13.18;
aspect ratio, 1.39.

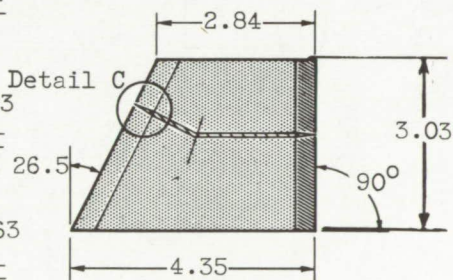
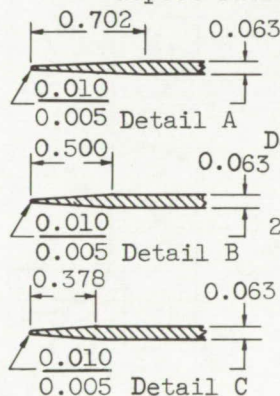


Fin E; fin area, 13.18;
aspect ratio, 1.39.

CD-3359

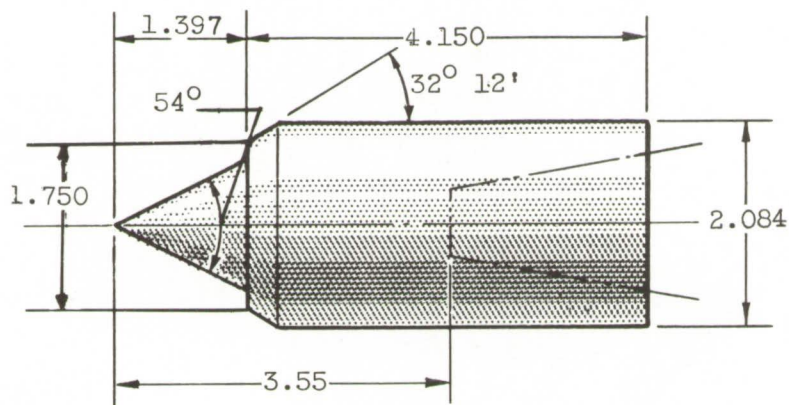
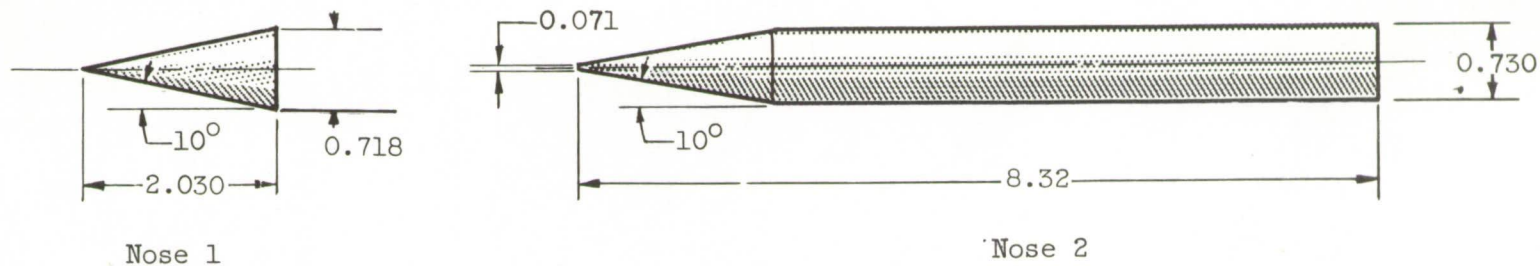


Fin F; fin area, 5.46;
aspect ratio, 2.31.



Fin C; fin area, 10.88;
aspect ratio, 1.69.

Figure 4. - Details of six fins tested. (All dimensions are in inches.)



CD-3359

Nose 3

Figure 5. - Details of three nose configurations tested. (All dimensions are in inches.)

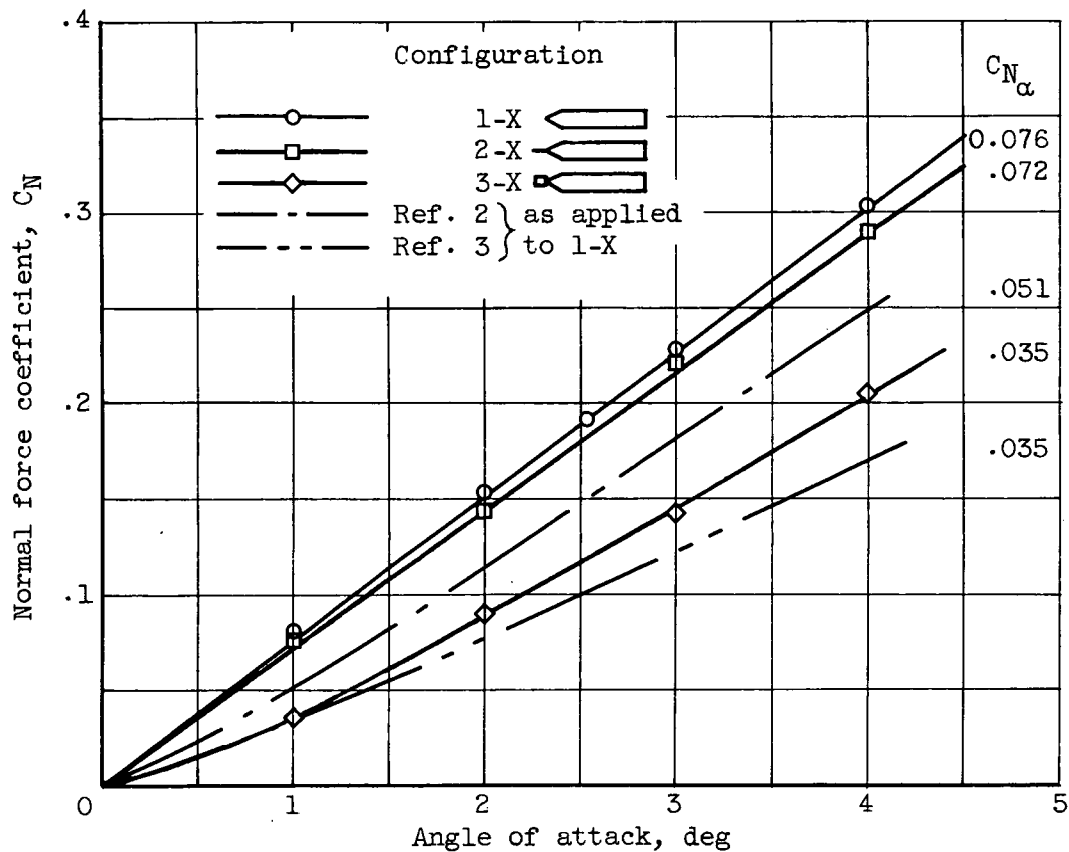
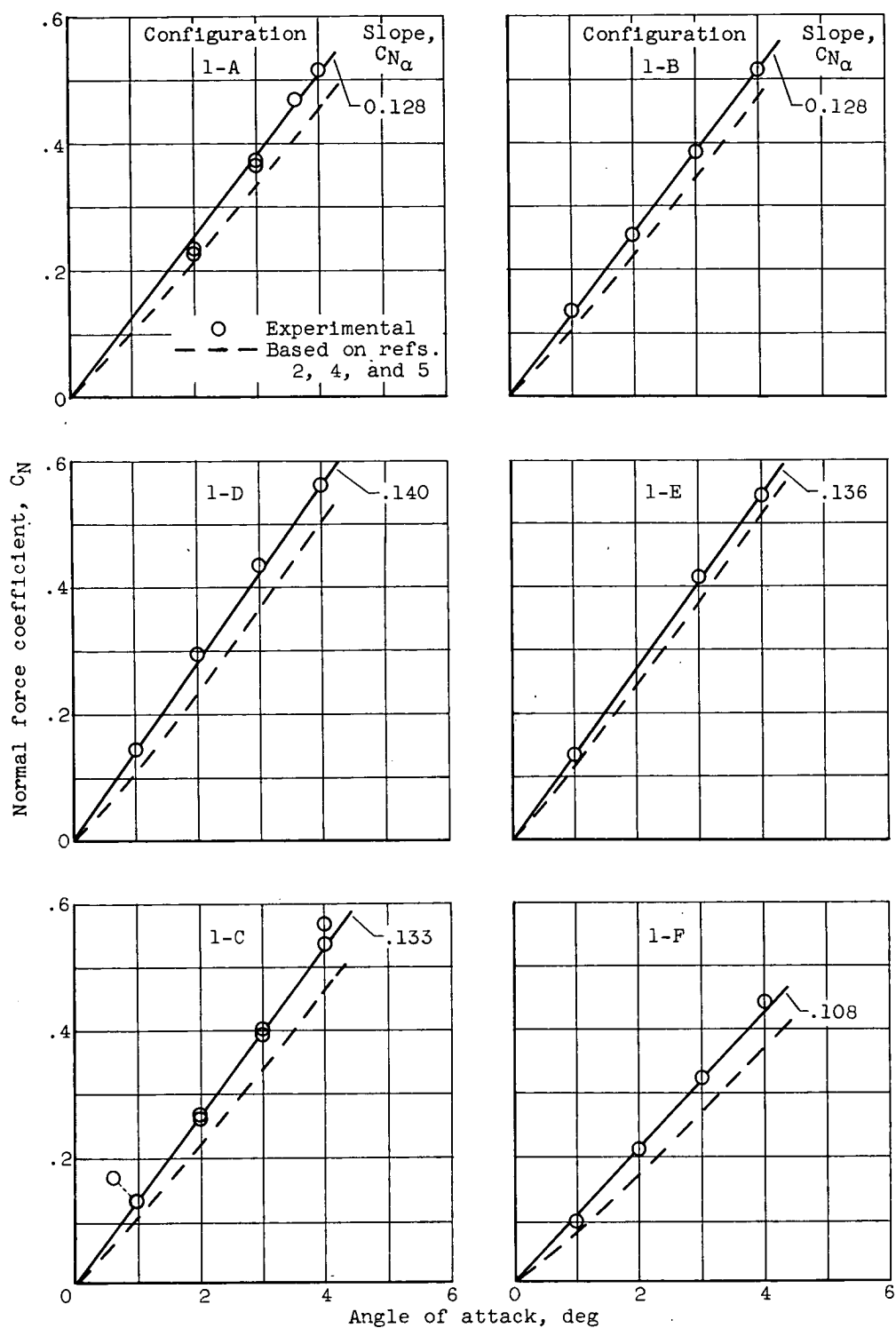
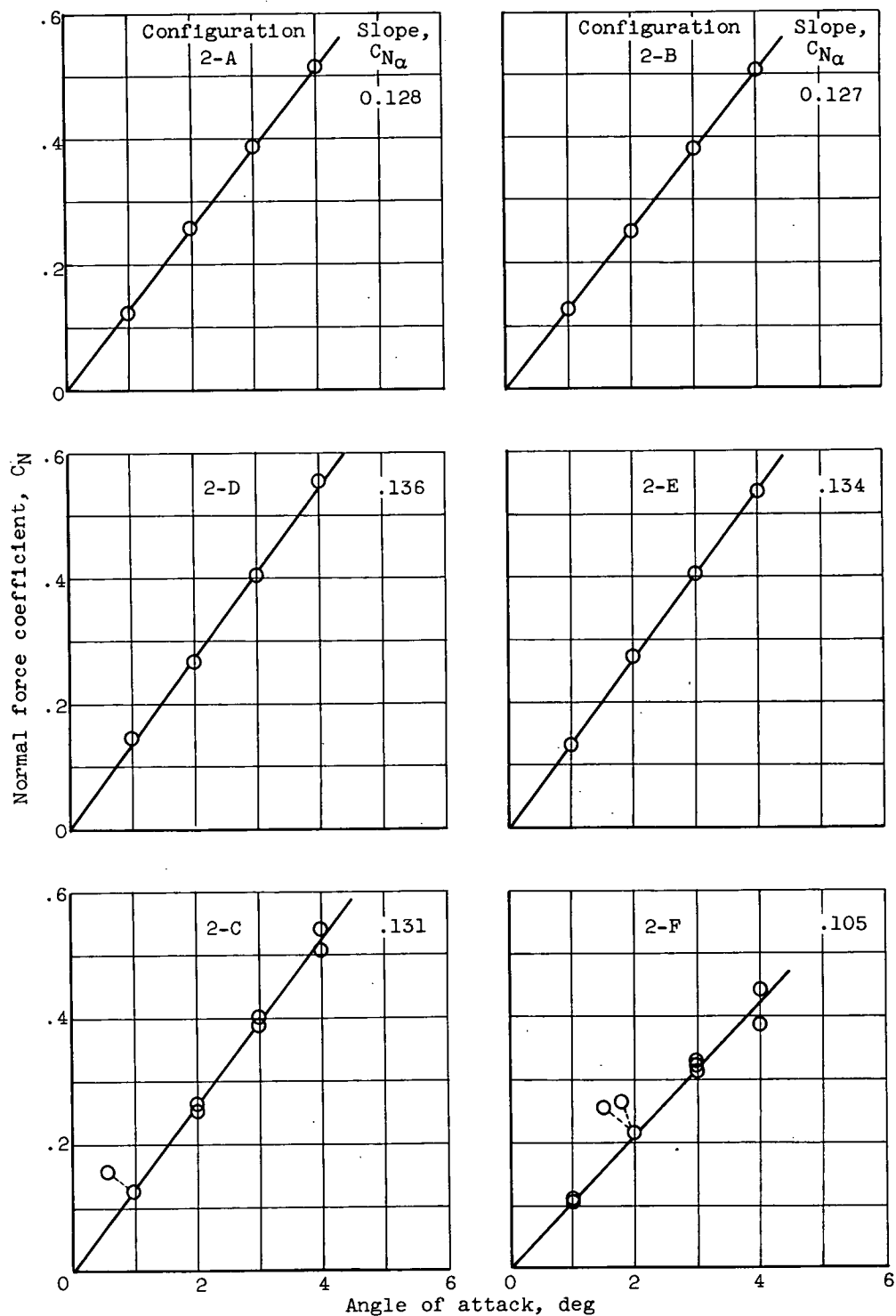


Figure 6. - Variation of normal force coefficient with angle of attack for body without fins.



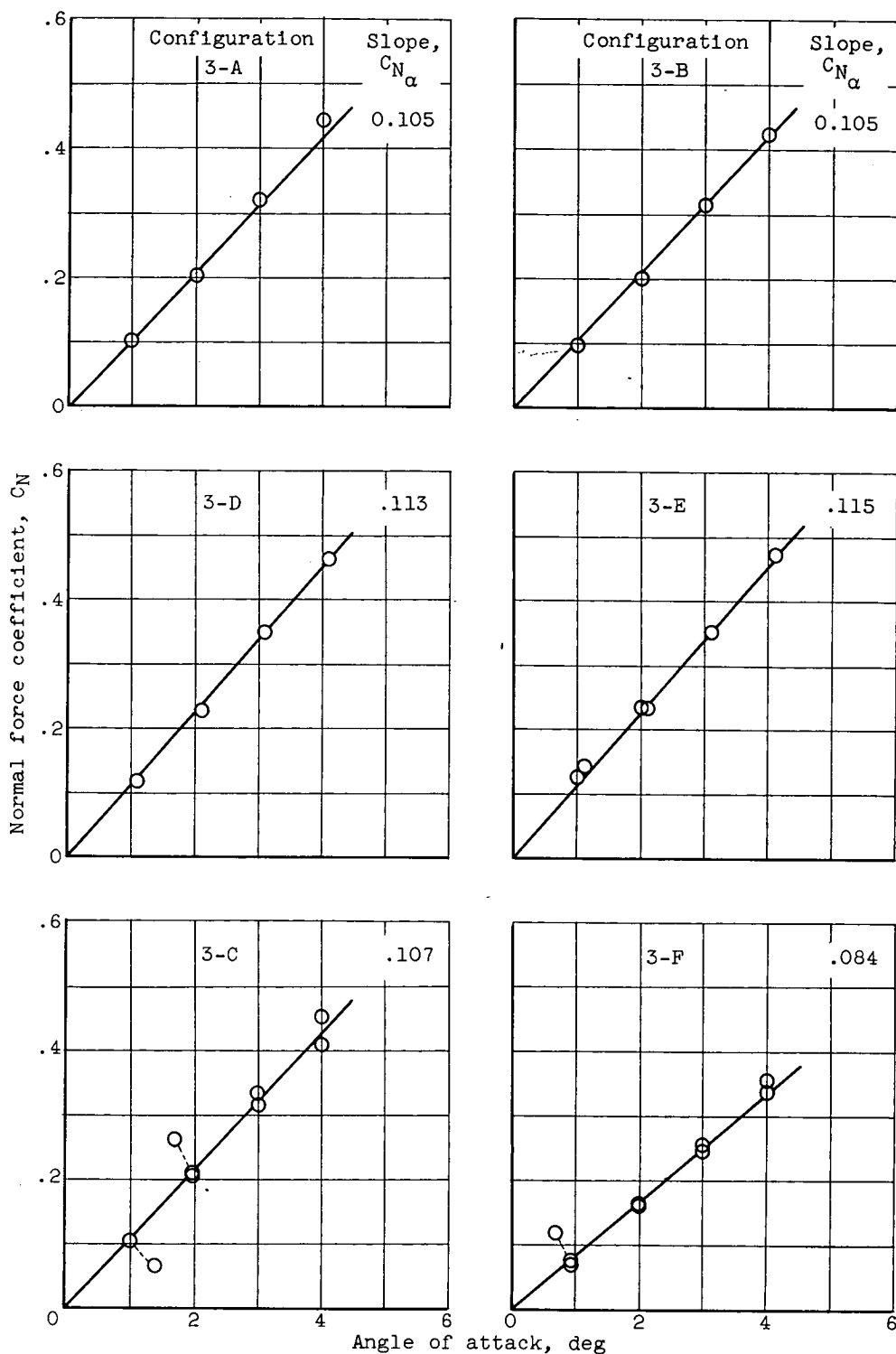
(a) Tested with nose 1.

Figure 7. - Variation of normal force coefficients of fin-body combinations with angle of attack.



(b) Tested with nose 2.

Figure 7. - Continued. Variation of normal force coefficients of fin-body combinations with angle of attack.



(c) Tested with nose 3.

Figure 7. - Concluded. Variation of normal force coefficient of fin-body combinations with angle of attack.

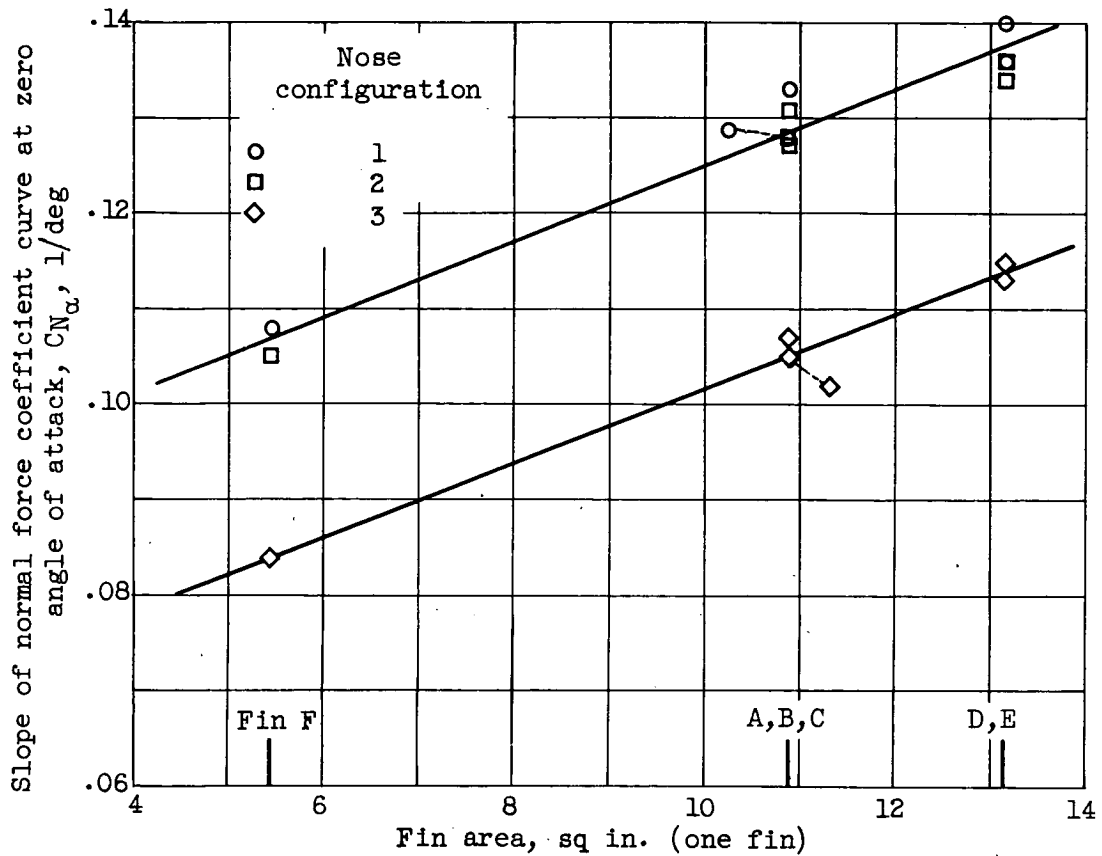
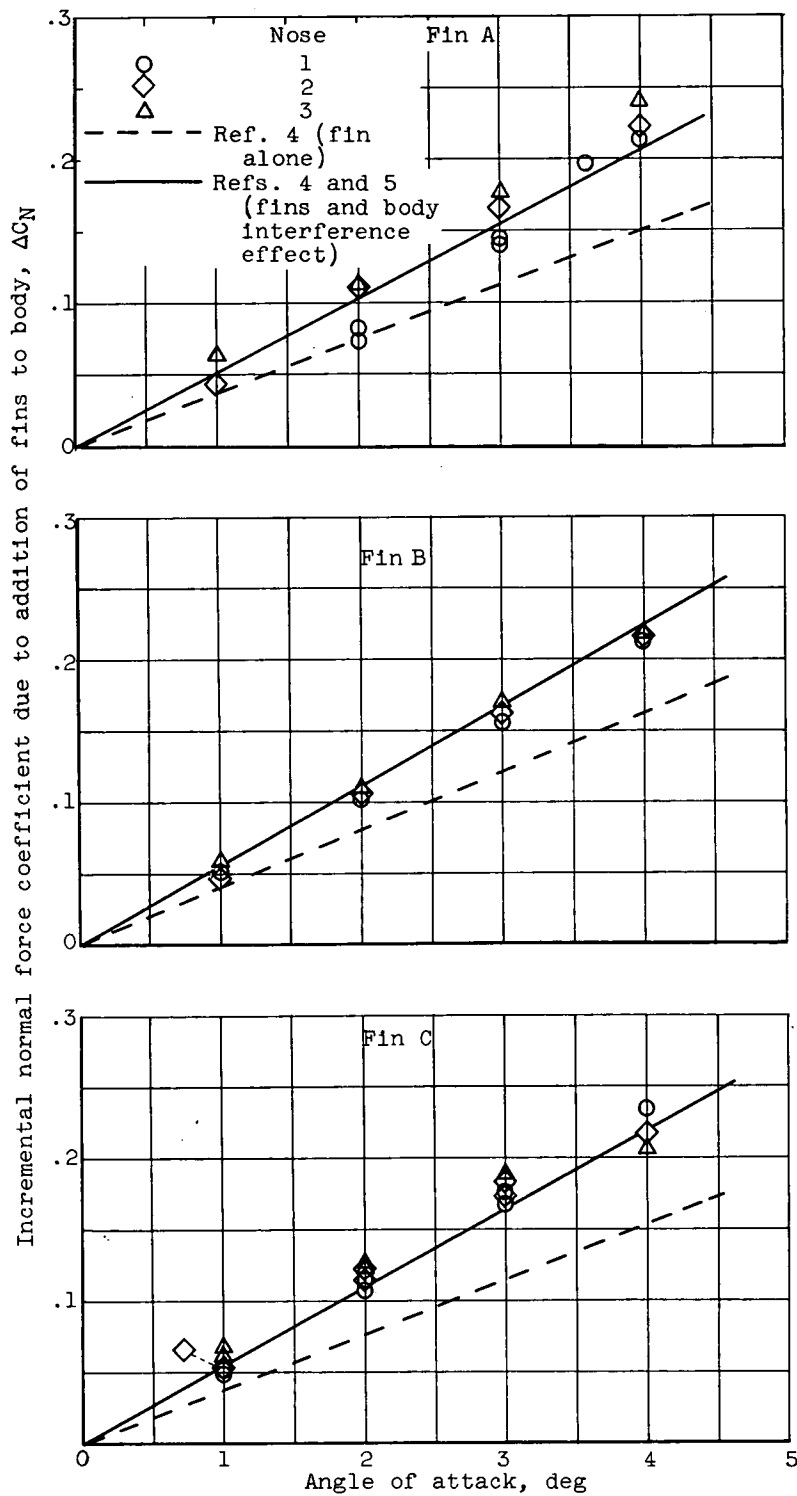
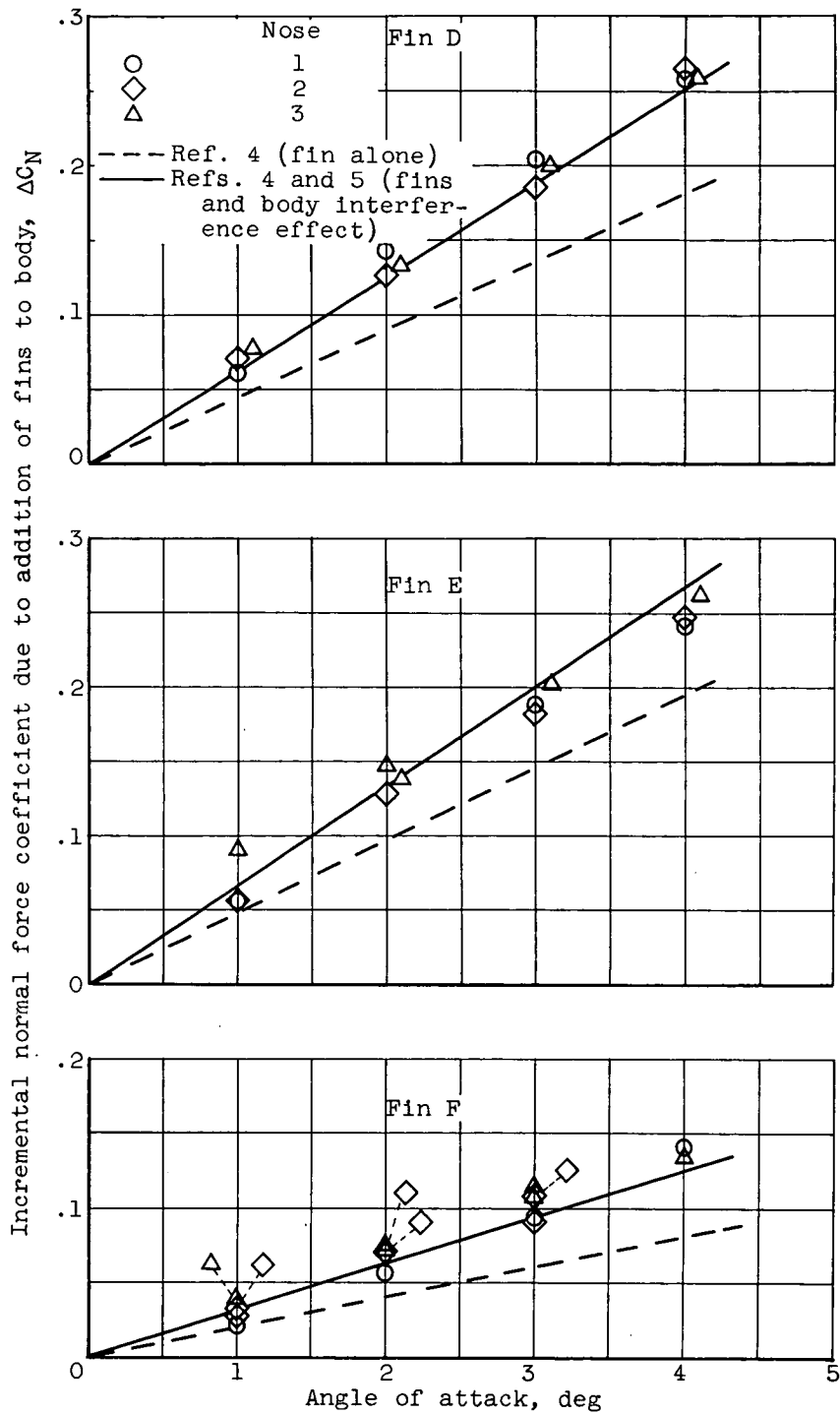


Figure 8. - Variation of slope of normal force coefficient curve at zero angle of attack with fin area.



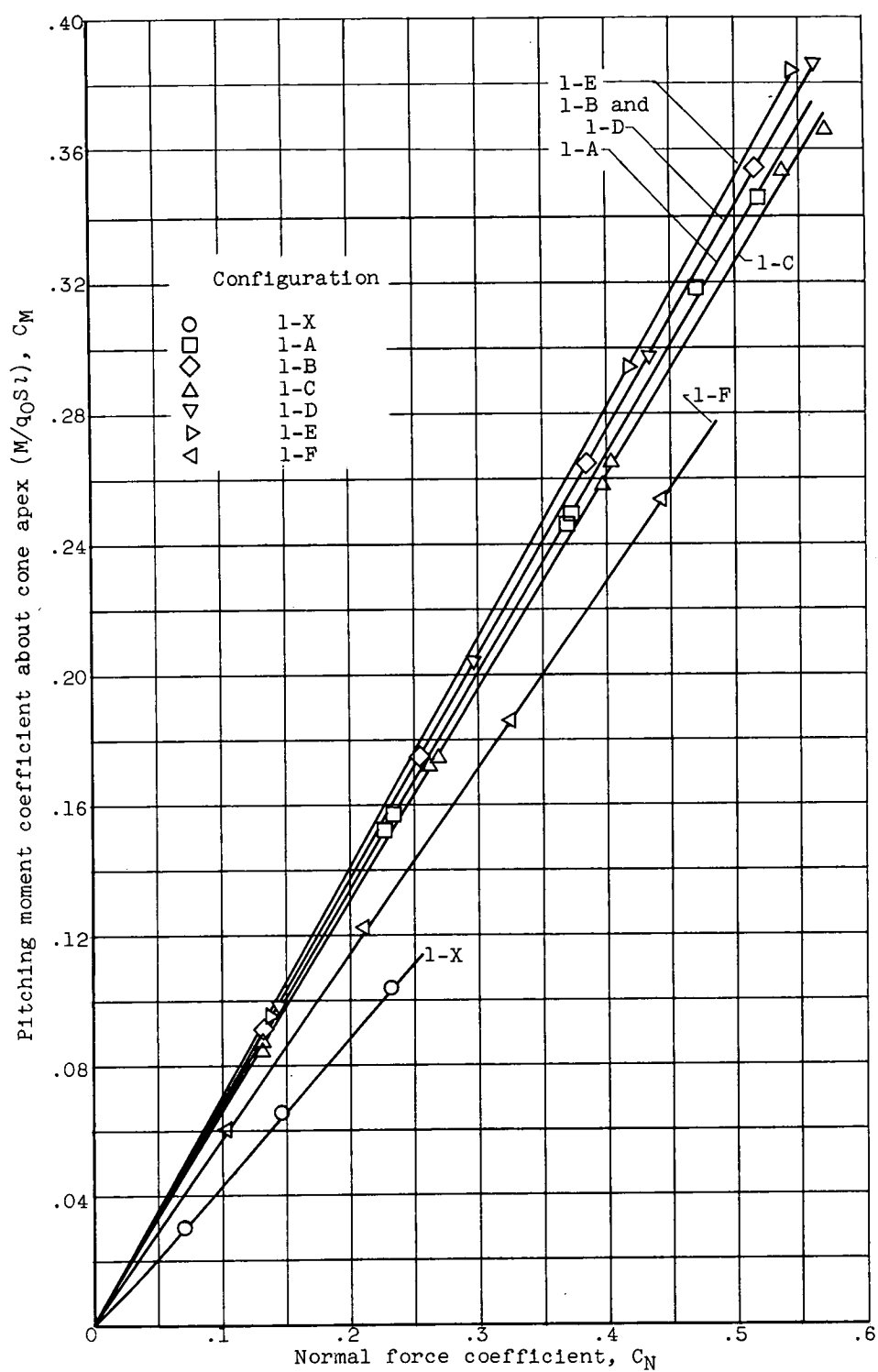
(a) Fins A, B, and C.

Figure 9. - Variation of incremental normal force coefficient ΔC_N with angle of attack.



(b) Fins D, E, and F.

Figure 9. - Concluded. Variation of incremental normal force coefficient ΔC_N with angle of attack.



(a) Nose 1.

Figure 10. - Variation of pitching moment coefficient with normal force coefficient for all configurations.

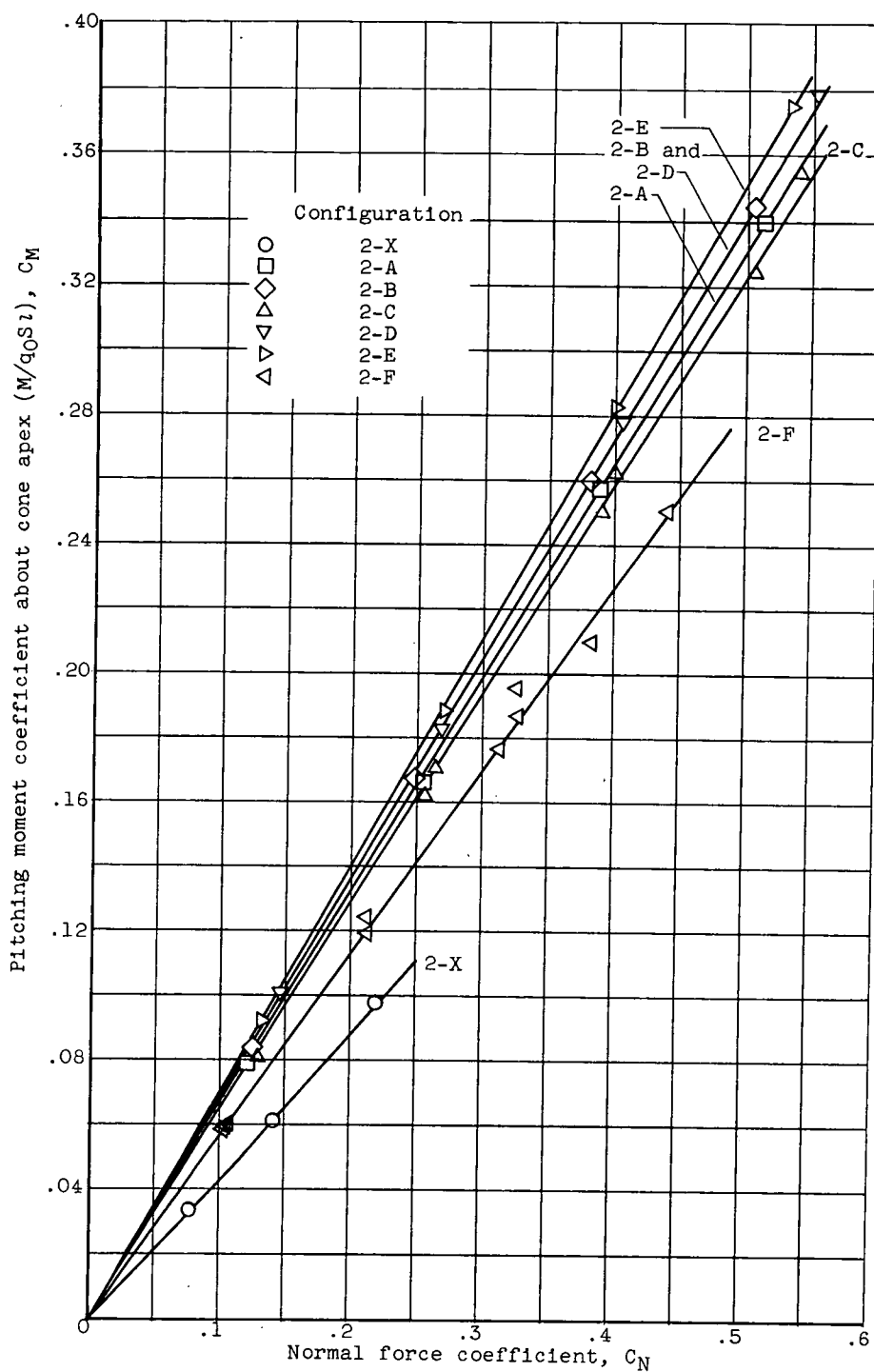


Figure 10. - Continued. Variation of pitching moment coefficient with normal force coefficient for all configurations.

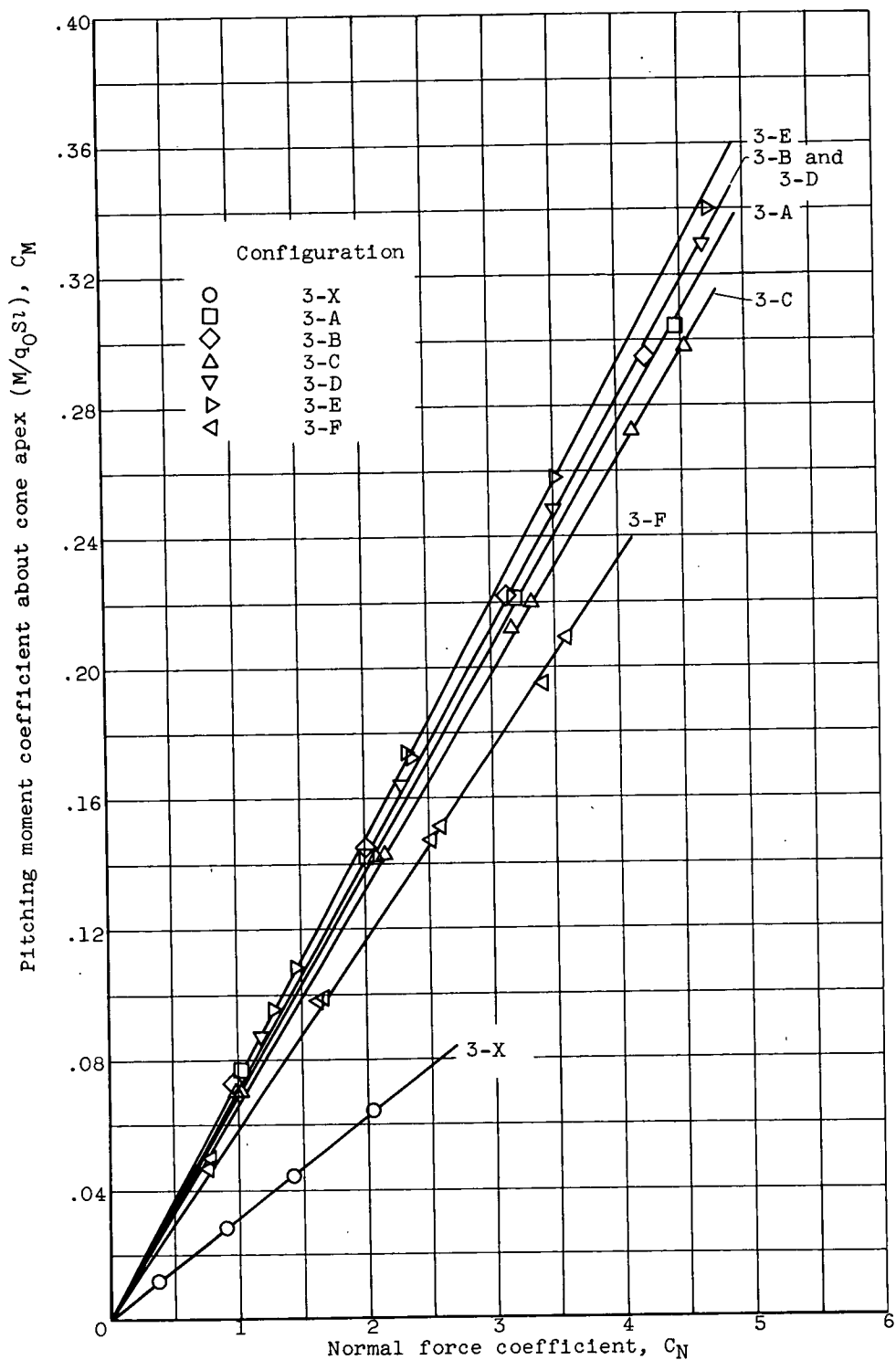
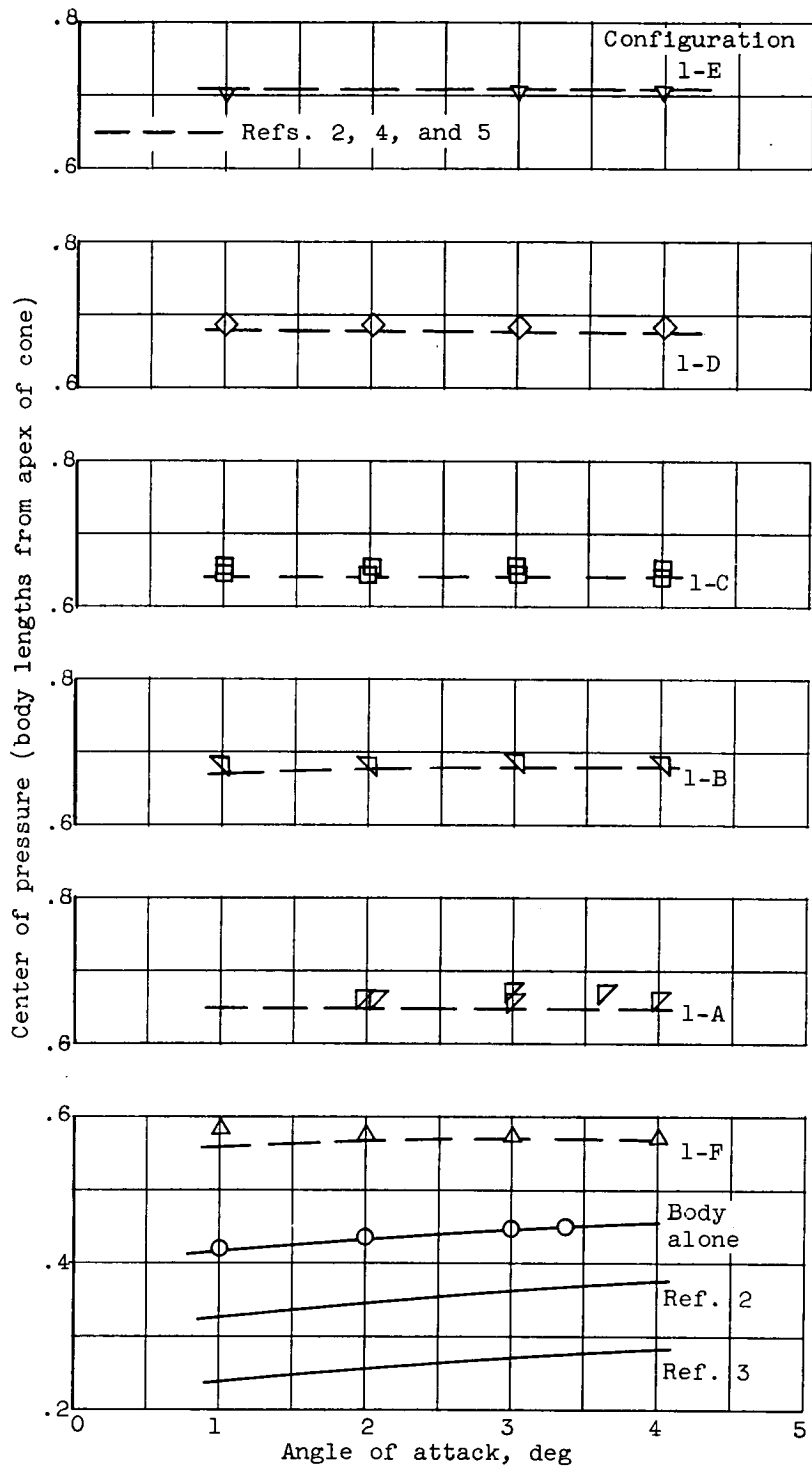
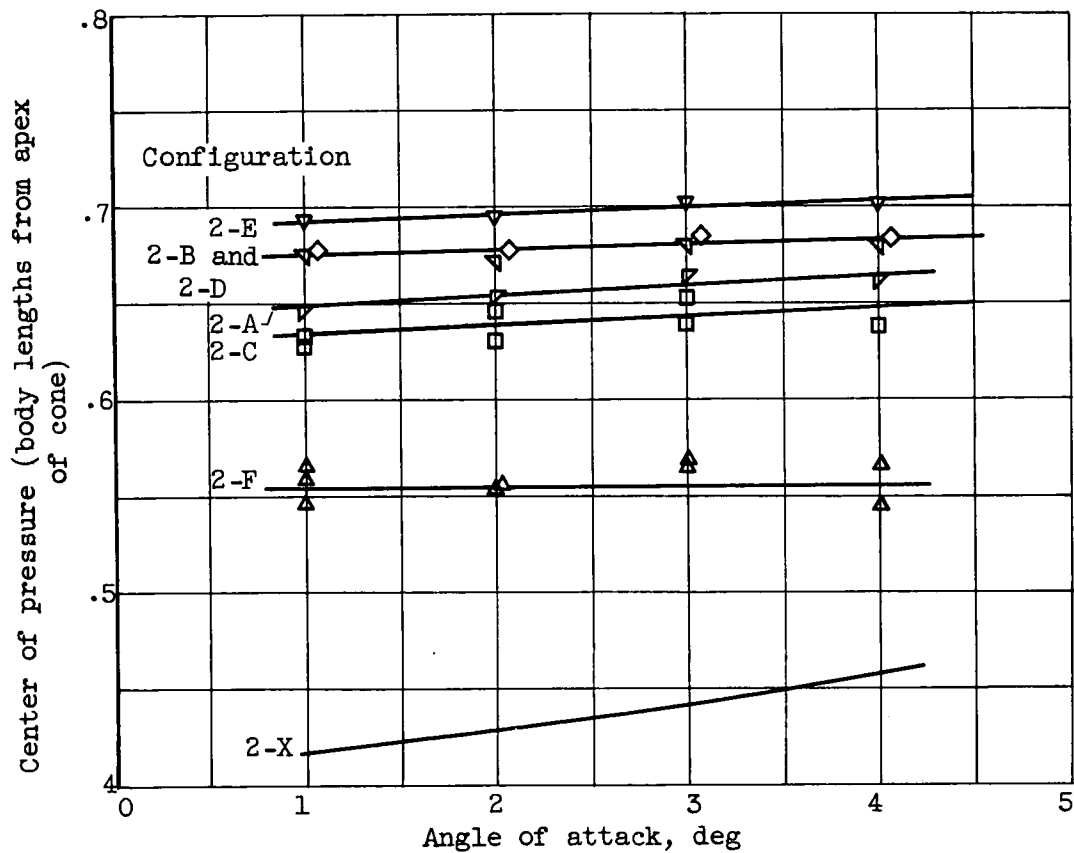


Figure 10. - Concluded. Variation of pitching moment coefficient with normal force coefficient for all configurations.



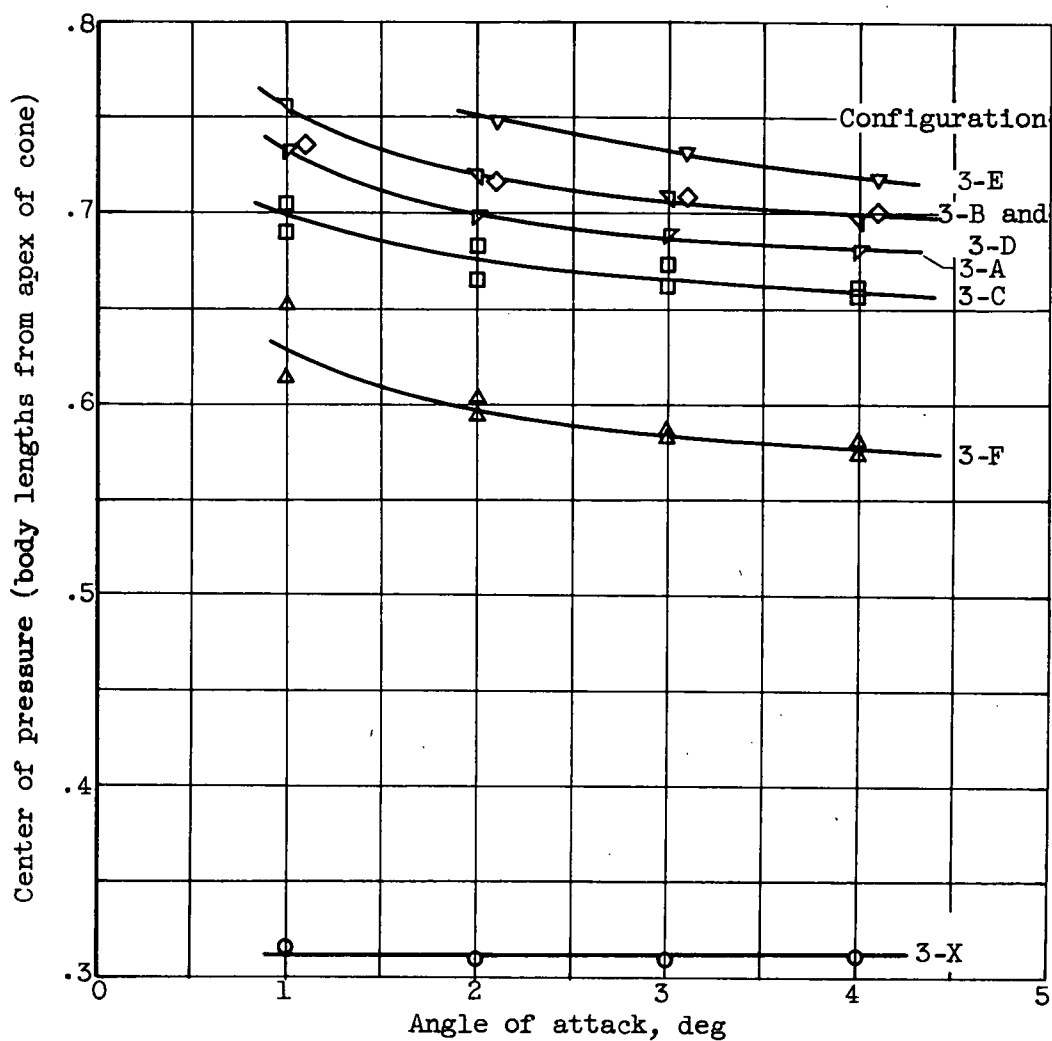
(a) Nose 1.

Figure 11. - Variation of center of pressure with angle of attack.



(b) Nose 2.

Figure 11. - Continued. Variation of center of pressure with angle of attack.



(c) Nose 3.

Figure 11. - Concluded. Variation of center of pressure with angle of attack.

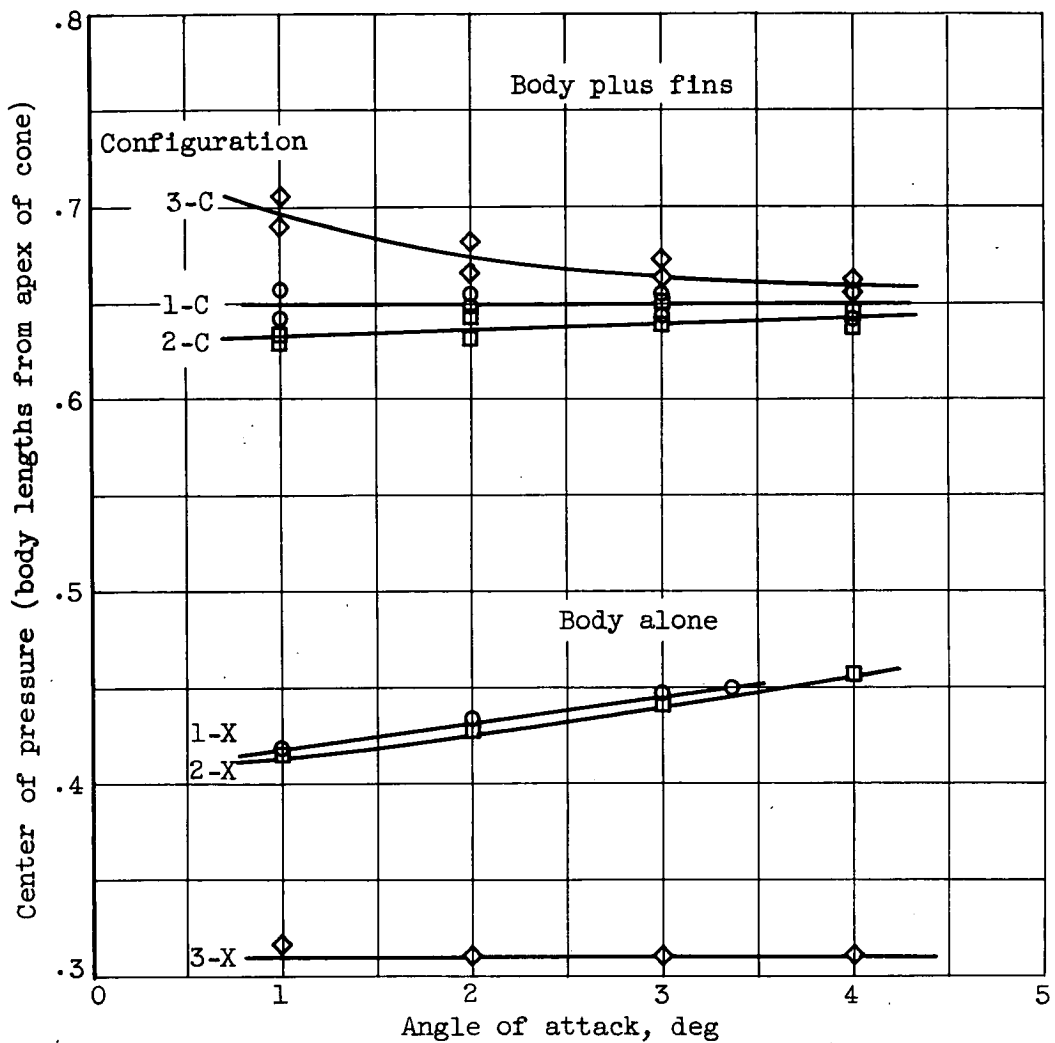


Figure 12. - Variation of center of pressure with angle of attack for bodies without fins and in combination with fin C.

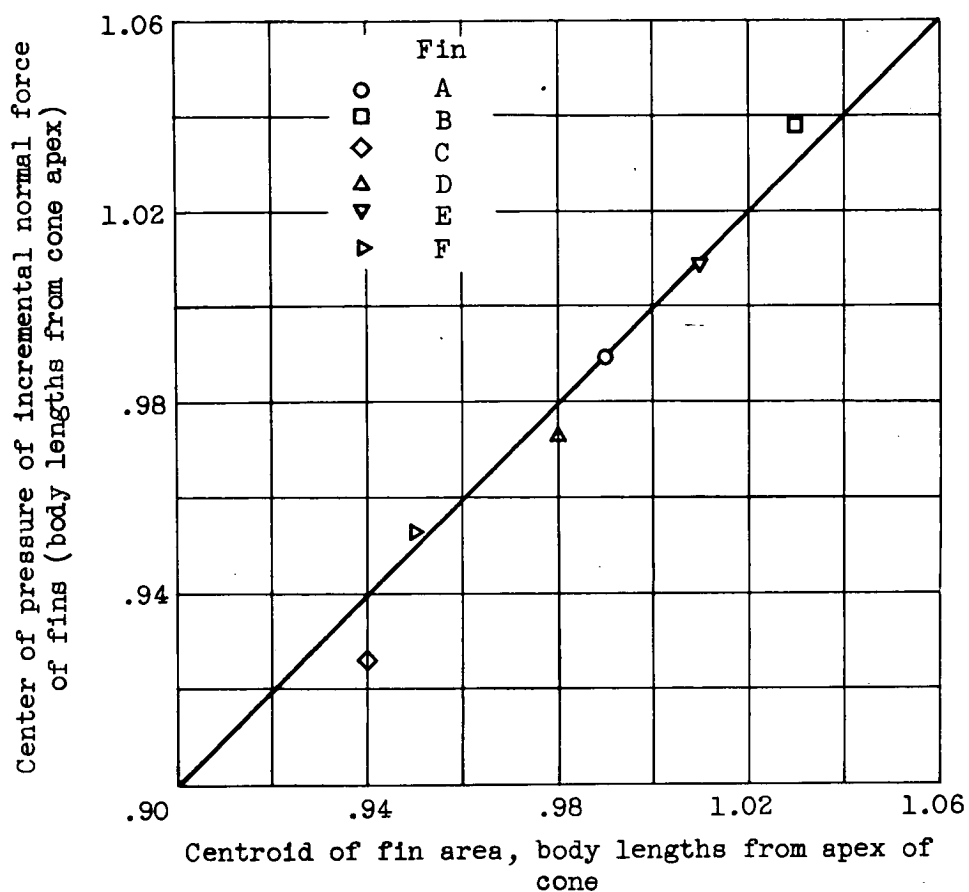


Figure 13. - Variation of center of pressure of incremental normal force of fins with centroid of fin area.